

# HEAVY LOAD, LOW TIRE PRESSURE RUTTING OF UNBOUND GRANULAR PAVEMENTS

By Robert A. Douglas<sup>1</sup>

(Reviewed by the Highway Division)

**ABSTRACT:** In a study of effects of wheels with very heavy loads but very low tire inflation pressures on unbound, single-layer granular pavements, trafficking tests were carried out on full-scale indoor pavements at the Pavement Test Facility, Transport Research Laboratory, Crowthorne, U.K. Two values of wheel load, two values of tire inflation pressure, and three subbase thicknesses were used. Testing was continued to 10,000 passes and a total of 4,704 measurements of rut depth made at intervals, providing a statistically significant data set. The development of ruts, the rut cross sections, and the effects of halving the tire inflation pressure or nearly doubling the wheel load are presented. Comparisons are made to a rut prediction equation derived by the U.S. Army Corps of Engineers Waterways Experiment Station in similar work, and conclusions are drawn.

## INTRODUCTION

The industrial forestry and mining access road "design environment" in North America is very different from the conventional public road design environment (Douglas 1998): gross vehicle masses and axle loads are at the legal limit where vehicles use public roads, and are far above the limit on private industrial roads; the terrain that access roads cross can be very hostile; and the cost ceiling for such transportation must be kept very low for the operations that the transportation systems serve to remain profitable. The desire to use extremely heavy vehicles on private roads for economic reasons, combined with very poor subgrade soils, presents acute problems for road designers. The problems are exacerbated by wet weather. Engineering solutions that at least reduce the severity of the problems and extend haul seasons even a week or two have a very beneficial impact.

One solution appears to be the use of central tire inflation (CTI), where a slow moving haul vehicle's tire pressure is deliberately greatly reduced in adverse conditions and then internally restored to normal in good conditions as the vehicle progresses along the haul. Trials have indicated that with reduced tire pressure, haul trucks have increased gradability, need not reduce payload in adverse conditions, require far less maintenance, do far less damage to the roads, and, indeed, may even "heal" previously damaged roads.

Numerous field demonstrations of CTI have been carried out by the U.S. Forest Service (USFS) and the U.S. Army Corps of Engineers. However, no determination of the actual mechanism for the behavior of the roads has yet been published.

Bekker (1956) demonstrated that tire footprints that are long relative to their width create lower stresses in soil than do short, wide footprints. Recent radial tire developments have produced tires capable of developing the desired long footprint at reduced tire inflation pressure. Ashmore and Sirois (1987) showed that while primarily a concept exploited by the military, CTI systems have been little used in civil applications. Czako (1974) listed 31 systems used in military applications

up to 1970. These were used predominantly on three-axle army trucks. Improved traction, drawbar pull, and gradability were observed when CTI systems were employed.

The USFS embarked on CTI research with a study of road damage mechanisms (Della-Moretta and Hodges 1983) and proof-of-concept tests at the San Dimas Equipment Development Center in 1984 (Della-Moretta, undated). Encouraged by the early results, the USFS set up field demonstrations in Idaho and Washington (Taylor 1987, 1988) and carried out additional trials in Alabama (Ashmore and Sirois 1987). While no mechanism for the road behavior was presented, it was demonstrated that CTI decreased road damage dramatically and significantly improved vehicle performance under adverse conditions.

The work led to an Interim Tire and Rim *Design Guide* for USFS CTI tests (1989) and a draft standard for CTI systems used on hauls under USFS control ("Standard" 1990). The necessary hardware is now readily available.

USFS work continued with trials at a test track at the Waterways Experiment Station in collaboration with the U.S. Army Corps of Engineers (Greenfield 1992; Murphy and Martin 1992). The work is reported in detail in Grau (1993) and Smith (1993). For granular surfaced roads, Grau (1993) observed better performance with low pressure tires in terms of reduced grading requirement, although on horizontal curves there was no noticeable difference in the performance of road sections subjected to different tire inflation pressures.

In Canada, the Forest Engineering Research Institute of Canada (FERIC) conducted preliminary trials on CTI (Bradley 1991). Subsequent results reported by Bradley (1992, 1993) and by Amlin and Bradley (1992) generally agreed with previous results.

To carry the research further, a series of well-controlled, instrumented tests was designed. The Transport Research Laboratory (TRL), Crowthorne, Berkshire, U.K., was contracted to carry out a full-scale study of the problem. TRL's Pavement Test Facility was used to conduct indoor tests on single-layer, unbound granular pavements constructed on a clay subgrade. The objectives were

- To track the development of ruts in the pavements with trafficking as a function of wheel load, tire inflation pressure, and subbase thickness, and to check these results against published design methods
- To make a preliminary examination of the "equivalent axle load" concept with respect to "unbound" flexible pavements
- To determine if the improved performance of such pave-

<sup>1</sup>D. C. Campbell Chair for Hwy. Constr. and Pavement Res., Dept. of Civ. Engrg., Univ. of New Brunswick, Fredericton, NB E3B 5A3, Canada.

Note. Discussion open until March 1, 1998. To extend the closing date one month, a written request must be filed with the ASCE Manager of Journals. The manuscript for this paper was submitted for review and possible publication on March 7, 1995. This paper is part of the *Journal of Transportation Engineering*, Vol. 123, No. 5, September/October, 1997. ©ASCE, ISSN 0733-947X/97/0005-0357-0363/\$4.00 + \$.50 per page. Paper No. 10457.

ments subjected to traffic by tires at very low inflation pressure was due to differences in the stresses and/or strains induced in the subgrade

This paper is concerned with the first objective. Subsequent papers will deal with the other objectives.

The design of the first phase of the experiment centered on tests with two wheel loads and two tire inflation pressures on roads with three subbase thicknesses. Six wheel paths were tested. Test road sections were constructed from June 29 through July 11, 1994, and the Phase I testing reported on here ran from July 20 to September 23, 1994.

## EXPERIMENT DETAILS

### Apparatus

The road structures were subjected to repeated passes  $N$  of the wheel load, up to a maximum of  $N = 10,000$  passes, in an effort to evaluate the progress of rut development. Loading was accomplished in the  $25 \times 10 \times 3$ -m-deep pit using a full-scale dual wheel assembly running beneath the heavy gantry in TRL's indoor facility (Fig. 1). The system is arranged with computer control of wheel load and travel speed, number of passes, and indexing (where the precise path of the tires can be varied transversely as much as  $\pm 0.5$  m from centerline for any given number of passes). The loading system allows the tires to comply with unevenness in the pavement surface to a maximum vertical travel of  $\pm 80$  mm. Wheel load is dynamically controlled to a tolerance  $\pm 2\%$  and a capacity of 100 kN is available. Speed is controlled to  $\pm 0.25$  km/h and a maximum of 20 km/h can be achieved. Wheel load and speed are sampled at 100 Hz and automatically adjusted, if required, "on the fly." Three values of each plus their averages are displayed and recorded for each pass. Should the system be unable to keep the load and speed within the set requirements, feedback systems automatically stop the run.

Tubeless radial tires, Dunlop model SP111MK, size designation 11.00 R 20, were mounted on a dual wheel on the loading carriage. Tire inflation pressures of as much as 830 kPa are not uncommon in conventional commercial applications, while central tire inflation systems permitting reduction of the inflation pressure for heavily loaded tires to 310 kPa have been reported. Using these values as a guide, a high value of 690 kPa was chosen, a common value used in commercial operations. A low value of 345 kPa was chosen because it was a reasonable approximation of the low values used in commercial central tire inflation settings, while at the same time it satisfied concerns about observed scuffing by the sidewalls of the adjacent tires on the dual wheel, causing the risk of heat buildup and tire failure. The inside walls of the tires just touched at this inflation pressure for the heavier load. Tire

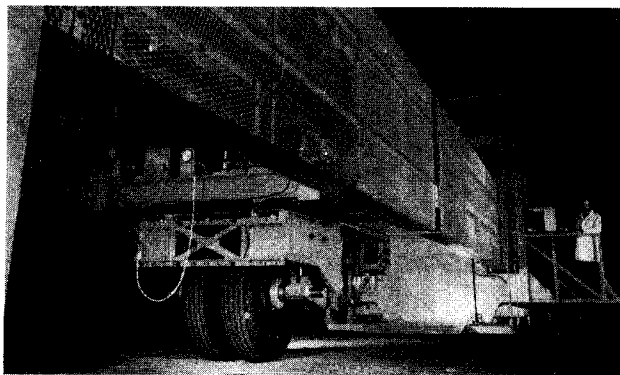


FIG. 1. Test Apparatus in TRL Pavement Test Facility [Photo: Transport Research Lab (TRL), Crowthorne, Berkshire, U.K.]

TABLE 1. Tire Deflections, Tires on Rigid Surface

Wheel load (kN) (1)	TIRE INFLATION PRESSURE (kPa)			
	345		690	
	Height* (mm) (2)	Deflection (%) (3)	Height* (mm) (4)	Deflection (%) (5)
0	22.5	—	22.5	—
44	18.8	17	19.8	12
80	15.0	33	18.2	19

\*Measured from rim down to rigid road surface.

TABLE 2. Wheel Load and Tire Inflation Pressure Designations

Tire inflation pressure (kPa) (1)	Wheel Load (kN)	
	44 = "w" (2)	80 = "W" (3)
345 = "p" 690 = "P"	wP WP	WP WP

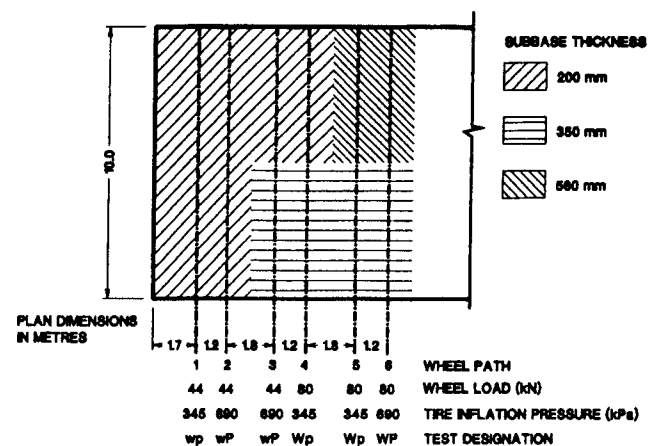


FIG. 2. Plan View of Test Pavements

deflections for the four combinations of wheel load and inflation pressure, when the tires were sitting on a rigid surface, are given in Table 1.

The selection of the two values for wheel load was based on standard Canadian practice and the maximum capacity of the test apparatus. Most jurisdictions in Canada permit a maximum of 44 kN per wheel (9 t per axle). Therefore, the "standard" wheel load for the experiment was set at this value and the high value of wheel load was set at 80 kN, i.e., about double the standard wheel load and near the capacity of the test facility. Four combinations of wheel load and tire inflation pressure therefore result. Table 2 shows the values and the test designation for each.

The pavements were constructed of a pit run material in a single layer on a clay subgrade 2.5–2.8-m-deep. The nominal subbase thicknesses were 200, 350, and 560 mm, representative of the range of subbase thicknesses encountered in access roads. Fig. 2 indicates the plan dimensions of the test pit, the areal extent of each thickness of subbase, and the wheel load and tire inflation pressure assigned to each of the six wheel paths.

### Clay Subgrade

The subgrade material was a medium Gault clay with a clay content ( $-2 \mu\text{m}$  size) of 52%. Plasticity tests indicated a plastic limit of 27, liquid limit of 55, and a plasticity index of 28. The soil was classified as CH according to the Unified Soil

classification system and as A-7-6 (20) according to the American Association of State Highway and Transportation Officials (AASHTO) classification system. Laboratory moisture-unit weight testing gave a standard Proctor maximum dry unit weight of 15.7 kN/m<sup>3</sup> at an optimum water content of 24%.

The subgrade material was placed and compacted in layers not exceeding 100 mm using small-scale self-propelled equipment. In-situ nuclear density testing gave an average dry unit weight of 15.3 kN/m<sup>3</sup> (with a standard deviation of 0.5 kN/m<sup>3</sup>, 64 observations) at an average water content of 23.5% (standard deviation 1.1%, 64 observations), implying compaction of 97% of standard Proctor maximum dry unit weight. In-situ California Bearing Ratio (CBR) tests gave average  $CBR_{subgrade} = 8.3$  (standard deviation of 1.6 for 19 observations).

### Granular Subbase

The pit run material used in the unbound road subbase was specified to conform to the United Kingdom Department of Transportation (UKDoT) standard for Type II granular subbase material ("United" 1991). Particle shape was subangular; surface texture was rough. Grain size distribution tests indicated a maximum nominal aggregate size of 50 mm, a fines content (-75 μm size) of 7.8%, a coefficient of uniformity  $C_u = 42$ , and a coefficient of curvature  $C_c = 4.5$ . The material was classified as GP-GM and A-1-a (0). Proctor tests are not meaningful for such coarse material, so they were not performed.

The same lightweight equipment used to compact the subbase material achieved an average in-situ dry unit weight, as determined by nuclear density testing, of 20.0 kN/m<sup>3</sup> (with standard deviation of 0.6 kN/m<sup>3</sup>, 112 observations), at an average water content of 2.7% (standard deviation of 0.8%, 112 observations). Laboratory CBR tests performed at various dry unit weights produced a CBR of 40 for a dry unit weight of 20.0 kN/m<sup>3</sup>.

It can be concluded from the results of geotechnical testing that both the subgrade and subbase of the test road were extremely uniform and consistent, much more so than would be expected at field sites.

### Data Collection Routine

Initial data collected included the unit weight and water content of the subbase and subgrade by nuclear density methods and the surveyed level data for the top of finished subgrade and the finished subbases.

Since the ruts were expected to develop roughly linearly with the logarithm of the number of wheel passes  $N$ , the data collection routine was organized so that trafficking was stopped for a day for intermediate measurements to be taken at  $N = 10, 30, 100, 300, 1,000, 3,000,$  and  $10,000$  passes. Testing at each intermediate stage included rut depth measurement by straightedge and wedge and by optical level survey, falling weight deflectometer (FWD) testing, dynamic cone penetration (DCP) testing, and Clegg rebound hammer testing on the surface of the subbase. Only the optical level survey results are dealt with here; the straightedge and wedge technique was simply used as a rapid check on rut development as testing proceeded, and subsequent papers will deal with the subbase and subgrade response, including the FWD, DCP, and Clegg results, together with dynamic subgrade stress and strain measurement.

The level survey of each wheel path entailed taking optical readings to the nearest 1 mm on a rod whose smallest unit was 1 cm at 0.5-m intervals along seven survey lines running parallel to the direction of wheel travel, spaced at 175-mm intervals across the wheel path. This transverse spacing placed five level lines within the coverage of the tire passes and two

outside it. At each stage of the testing, 588 readings (six wheel paths × seven survey lines per wheel path × 14 observations per survey line) were taken. The complete set of levels for rut depth determination totals 4,704 readings, providing a body of data large enough for statistically significant treatment of the observations. Positive rut depth at an observation point was defined as a lowering of the subbase surface at that point compared to its original level prior to any trafficking.

### OBSERVED RUT DEVELOPMENT

The middle five survey lines for each wheel path were used to determine rut depths. These were averaged for each com-

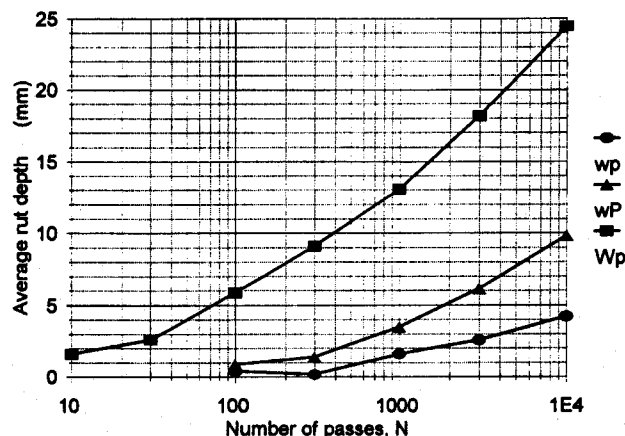


FIG. 3. Average Rut Depth versus  $\log(N)$ , 200-mm-Thick Subbase

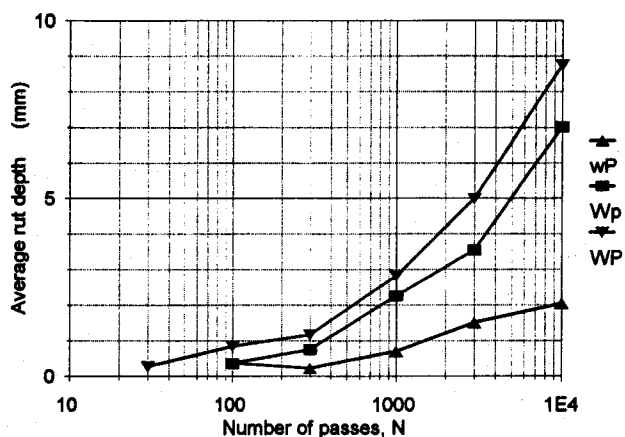


FIG. 4. Average Rut Depth versus  $\log(N)$ , 350-mm-Thick Subbase

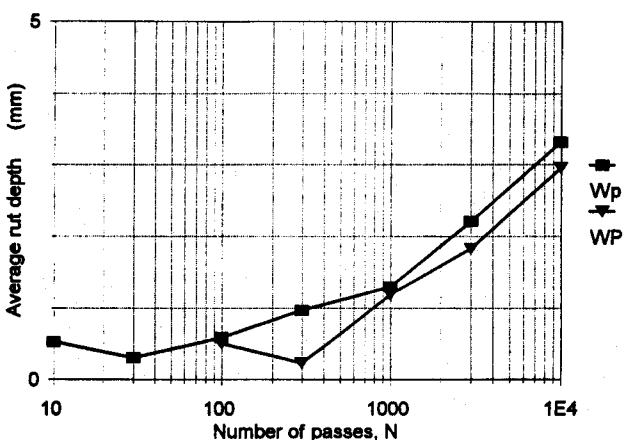


FIG. 5. Average Rut Depth versus  $\log(N)$ , 560-mm-Thick Subbase

bination of wheel load and tire inflation pressure for the half lengths of each wheel path, from 0 to 5 m or 5 to 10 m. The calculation was made for each level of traffic. Given that there was some duplication for certain combinations of wheel load and tire inflation pressure, the rut depths were further averaged by wheel load/tire pressure/subbase thickness combination.

The calculated average rut depths, as a function of  $\log(N)$ , are plotted for each wheel load/tire inflation pressure combination in Figs. 3–5. In all cases, the curves are nonlinear with the rate of rut development steadily increasing with  $\log(N)$ .

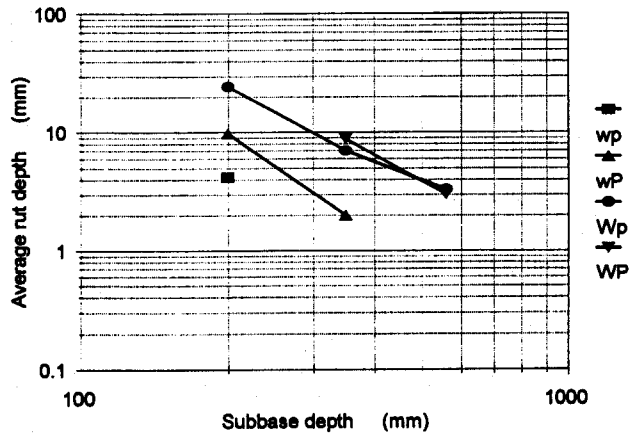


FIG. 6. Log (Average Rut Depth) versus log (Subbase Thickness),  $N = 10,000$  Passes

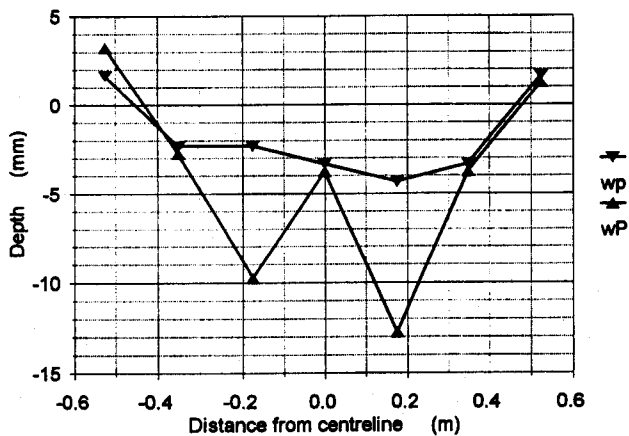


FIG. 7. Typical Rut Cross Sections for 200-mm-Thick Subbase,  $N = 10,000$  Passes, and 44-kN Wheel Load: Low Inflation Pressure = 345 kPa (Wheel Path 1 at 6.0 m), High Inflation Pressure = 690 kPa (Wheel Path 2 at 3.5 m)

The results are plotted as the logarithm of the average rut depth against the logarithm of the subbase thickness for the relevant combinations of wheel load and tire inflation pressure for  $N = 10,000$  passes in Fig. 6.

## RUT SHAPE

It was postulated that the tire inflation pressure would have an effect on the shape of rut that would be developed. In particular, it was anticipated that the road sections subjected to the more cutting action of tires at the higher inflation pressure (690 kPa) would develop more rounded ruts, even despite the fact that the wheel paths were indexed every 10 passes during the trafficking, and the indexing was wide enough to ensure full overlapping of the paths taken by individual tires. It was expected that a greater variation would be observed in the level survey results for those wheel paths where the tire inflation pressure had been at the higher value than would be the case for ruts formed by tires at the lower inflation pressure. Fig. 7 gives an indication of what was observed. It can be seen that the lower tire inflation pressure caused a flatter rut cross section with no peak in the center.

A measure of the variability of the observed levels across a rut cross section is the standard deviation of the readings. Table 3 shows the standard deviations of the observed rut depths for the middle five survey lines for each wheel path. The two outside survey lines, beyond the tire coverage, were ignored in the calculation for each wheel path.

## EFFECT OF "DOUBLING" WHEEL LOAD OR HALVING TIRE INFLATION PRESSURE

There are enough overlaps in the test configurations (wheel load/tire inflation pressure/subbase thickness combinations) that a preliminary look at the effects of nearly doubling the wheel load or halving the tire inflation pressure can be taken. Table 4 shows these results in the form of rut depth ratios, comparing the rut depth for the changed configuration to the baseline configuration. Only those rut depths greater than 1 mm were permitted in the calculation because it was thought that measured rut depths less than 1 mm were below the accuracy of the optical survey procedure performed on the surface of the coarse subbase and would therefore be unreliable.

## DESIGN COMPARISON

Empirical equations have been developed from multiple regressions by the U.S. Corps of Engineers at the Waterways Experiment Station (WES). Of interest is the equation devel-

TABLE 3. Standard Deviations of Rut Readings on Middle Five Survey Lines of Each Wheel Path (mm)

Designation (1)	Subbase thickness (mm) (2)	Wheel path (3)	Distance along wheel path (4)	$N$							Average (12)
				10 (5)	30 (6)	100 (7)	300 (8)	1,000 (9)	3,000 (10)	10,000 (11)	
wp	200	1	0–5	1.10	1.13	0.98	1.30	1.48	1.59	2.33	1.42
wp	200	1	5–10	1.51	2.22	1.56	1.59	1.66	1.80	2.35	1.81
wP	200	2	0–5	0.99	1.40	1.58	1.85	3.11	3.61	4.73	2.47
wP	200	2	5–10	1.37	1.32	1.55	2.07	2.74	3.51	4.22	2.40
wP	350	3	0–5	0.92	1.13	1.25	1.04	1.52	1.70	1.67	1.32
wP	200	3	5–10	1.61	1.89	2.11	2.25	3.46	4.41	4.91	2.95
Wp	350	4	0–5	1.13	1.13	1.55	1.95	2.27	2.72	3.65	2.06
Wp	200	4	5–10	1.79	2.85	4.17	4.56	5.84	7.08	7.29	4.80
Wp	350	5	0–5	1.23	1.34	1.28	1.38	1.96	2.25	3.90	1.90
Wp	560	5	5–10	1.18	1.18	1.20	1.21	2.09	1.69	2.48	1.58
WP	350	6	0–5	1.15	1.09	1.68	1.63	2.30	3.19	4.39	2.20
WP	560	6	5–10	1.18	1.22	1.21	1.20	1.37	1.50	1.50	1.31

Note: Grand average, low inflation pressure = 2.26 mm; grand average, low inflation pressure, excluding wheel path 4, 5–10 m segment = 1.74 mm; grand average, high inflation pressure = 2.11 mm.

TABLE 4. Ratios of Average Rut Depths

Effect (1)	Subbase thickness (mm) (2)	Applicable ratio (3)	N			Average <sup>a</sup> (7)
			1,000 (4)	3,000 (5)	10,000 (6)	
"Doubling" wheel load <sup>b</sup>	200	Wp/wp	8.2	7.0	5.8	7.0
	350	WP/wP	—	3.3	4.3	3.8
Halving tire inflation pressure <sup>c</sup>	200	wp/wP	0.46	0.42	0.43	0.44
	350	Wp/WP	—	0.71	0.80	0.76
Halving tire inflation pressure <sup>c</sup>	560	Wp/WP	1.10	1.20	1.12	1.14

<sup>a</sup>Grand average for "doubling" wheel load at thicknesses of 200 and 350 mm = 5.7; grand average for halving tire inflation pressure at same thicknesses = 0.56.  
<sup>b</sup>W/w = 80/44 = 1.82.  
<sup>c</sup>p/P = 345/690 = 0.5.

oped in 1992 (Smith 1993), relating rut depth to various parameters

$$RD = (0.109) \times \frac{P_k^{0.499} t_p^{0.564} R^{0.242}}{(\log t)^{1.57} C_1^{0.917} C_2^{0.0365}} \quad (1)$$

where (in the original units presented, and with the range of values tested or observed) *RD* = rut depth (in.) (maximum observed, 5.62 in.); *P<sub>k</sub>* = equivalent single wheel load (kips) (maximum, 40 kips); *t<sub>p</sub>* = tire inflation pressure (lb/in.<sup>2</sup>) (20 < *t<sub>p</sub>* < 165 lb/in.<sup>2</sup>); *R* = number of passes (5 < *R* < 6,800 passes); *t* = subbase thickness (in.) (2.5 < *t* < 24 in.); *C<sub>1</sub>* = CBR for subbase [5.1 < *C<sub>1</sub>* < 132 (sic)]; and *C<sub>2</sub>* = CBR for subgrade (2.2 < *C<sub>2</sub>* < 21).

The validity of (1) for the test results here can be conveniently checked by comparison against the observed data.

**ANALYSIS**

**Average Rut Depth Development**

Interest in the rate of rut development in unbound single-layer granular roads has grown (personal communication, A. Dawson). Figs. 3–5 show curves that are all concave upwards on a rut depth-log(*N*) plot. It must be remembered that each point on these plots represents an average of at least 35 observations of rut depth for the given combination of wheel load, tire inflation pressure, and number of passes (and in certain cases more observations). Thus a great deal more confidence can be placed in them than the usually much less voluminous data obtained in field testing.

The ruts deepened exponentially with the number of passes. Rate of rut formation consistently accelerated from just a few passes up to 10,000 passes. The model roads were thus accelerating toward failure right from the earliest stages of trafficking.

It is seen in Fig. 6 that once a significant number of passes had been made (*N* = 1,000 passes), the data collected gave linear and parallel log(average rut depth) – log (*N*) curves. The plots are not as scanty as they might seem at first: each point represents an average of at least 35 observations of rut depth. Similar plots could be used as design charts for such pavements.

**Rut Shape**

Standard deviation is a measure of the variability of data; for a more rounded rut cross section, with a peak in the center, the levels observed on the five survey lines in a rut at any cross section would give more varied values than they would for a flat-bottomed rut and thus yield a higher calculated standard deviation. A perfectly flat-bottomed rut would yield a standard deviation of zero.

The expected rut shape difference depicted in Fig. 7 is amplified by Table 3, which gives the calculated standard deviation



FIG. 8. Anomalous Section: Wheel Path 4, 5–10 m, 200-mm-Thick Subbase, at *N* = 300 passes (Crosses on Road Surface are Spaced at 1 m on Center Along Wheel Path)

for each set of 35 observations of rut depth (five survey lines × seven rod positions in a half length of a wheel path per survey line) for a given combination of wheel load, tire inflation pressure, subbase thickness, and number of passes. There are 84 such combinations in the experiment.

Standard deviations were first averaged for *N* = 10, 30, 100, . . . , 10,000 to determine if there were any trends. Apart from the one anomalous average value of 4.80 for Wheel Path 4 at the segment running from 5 to 10 m (Wp, 200-mm-thick subbase), it appeared that the average standard deviation for a configuration was lower for the low tire inflation pressure configurations, regardless of wheel load, than it was for a high-pressure configuration. If the anomalous value is included, the grand averages of standard deviation are about the same for the low and high pressure configurations (2.26 and 2.11, respectively), with the low pressure grand average 7% higher (more variation in cross section) than the grand average for the high pressures. However, if the anomalous value is

dropped from the calculation, the grand average for the low inflation pressure configurations was 21% lower than the grand average for the high pressure configurations.

Apart from rejecting the anomalous value because it was more than double any other value in the data set the average standard deviations, it is reasonable to reject it because that particular model road section had been observed to have a deficiency of fines at the surface, making it more susceptible to raveling compared to other sections. Fig. 8 illustrated the condition of the surface at this location after 300 passes.

### “Doubling” Axle Load, Halving Tire Inflation Pressure

The data in Figs. 3–5, representing the average rut depth observed on each road segment (wheel path half length) at a given number of passes, was used to calculate rut depth ratios in Table 4. For a given subbase thickness, the design of the experiment permitted the comparison of rut depths for certain pairs of road segments that had the same wheel load but different tire inflation pressures, or vice versa. By taking the ratio of the average rut depths for some changed configuration divided by some control configuration, the effects of nearly doubling the wheel load while keeping the inflation pressure constant or halving the tire inflation pressure while keeping the wheel load constant can be assessed.

As shown in Table 4, increasing the wheel load by 82% caused, on average, ruts approximately 5.7 times deeper (ranging from 3.3 to 8.2 times deeper) to form, all else being kept equal. Having the tire inflation pressure resulted, on average, in causing ruts approximately 0.56 times the depth (ranging from 0.42 to 0.80 times the depth) to form. Data for ruts less than 1 mm were excluded from consideration because it was thought unreliable, given the measurement techniques used and the coarse material comprising the subbase.

In addition, the data for the 560-mm-thick subbase was excluded because, although the rut depths measured were indeed somewhat greater than 1 mm, a small reverse trend was observed, with the low inflation pressure observed to result in slightly deeper ruts. It was felt that this also reflected the level of precision in the rut readings, rather than some significantly different behavior in the thickest subbase.

Finally, taking the raw data and calculating a combined ratio representing the effect of increasing the wheel load by 82% while halving the tire inflation pressure gives a value of 3.0, close to the product of the grand averages in Table 4:  $5.7 \times 0.56 = 3.2$ .

### Check against Design Method

The validity of (1) produced by WES for predicting the observed data was checked by plotting the rut depth predicted by the equation against all the average rut depths calculated in Fig. 9. A perfect match would place the data points on the line drawn through the figure.

In Fig. 9, the results for Wheel Path 4, 5–10 m, do not fit well with the rest of the data. Recall that the material seen at the surface for that wheel path was deficient in fines (Fig. 8). An interpretation is that for that particular wheel path, for a given calculated rut depth using (1), the observed rut depths were greater than anticipated, based on the rut depths observed on other wheel paths. This may have been due to the loss of material from the surface on that wheel path.

If Wheel Path 4 data is removed from the data set, Fig. 10 results. It is seen that the remaining data points follow a strong trend. A regression analysis returned  $r^2 = 0.831$ , and intercept of 10 mm, and a slope coefficient of 4.03.

Eq. (1) overestimated the rut depths observed in all cases. This can be attributed to inherent variation in the observed

data, inappropriate input data, inaccuracy of the equation itself, or differing definitions of “rut depth.”

The variation in the observed data can be estimated by making reference to the standard deviations calculated for all levels in a given road section. Based on the data in Table 3, the standard deviation of the readings was as much as 3 mm. For an assumed normal distribution, 98% of the rut depths observed therefore would be within  $\pm 2.33$  standard deviations ( $\pm 7$  mm) of their averages. It is seen that most of the rut depths predicted by (1) are still more than 7 mm outside the “perfect fit line”, so it is concluded that the inherent variability of the data is not responsible for the difference.

With one exception, no interpretation of the input data was needed. Except for the wheel loads, observed field and laboratory data were input directly to (1). The WES formulation of the equation requires the input of an “equivalent single wheel load” (ESWL). The definition of ESWL has nothing to do with the more familiar 80-kN equivalent single axle load (ESAL). ESWL is derived from an “equivalent single wheel load factor” (ESWLF), calculated by a computer program available from WES. The program determines the equivalency by equating the vertical displacements at some depth, caused by the wheel group, to that which would be caused by a single tire of the same type.

It is important to note that ESWLF varies with depth. In the solution of (1), the depth selected was equal to the subbase thickness on the assumption that the greater proportion of the

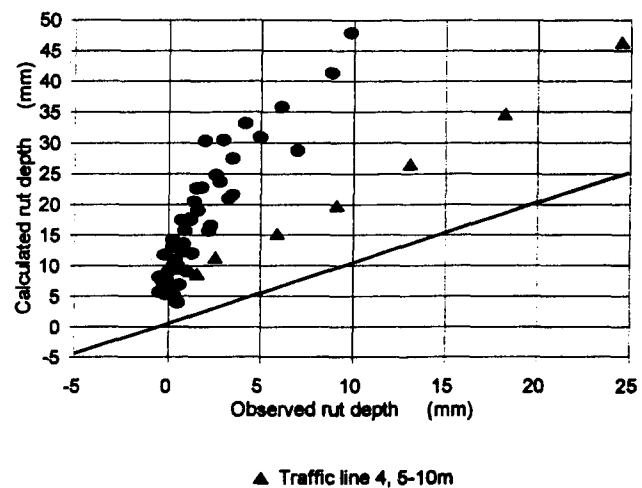


FIG. 9. Comparison of Corps of Engineers 1992 Equation Predictions for Rut Depth to Observed Rut Depth for All Data; Triangle Symbols Are for Wheel Path 4, 5–10 m

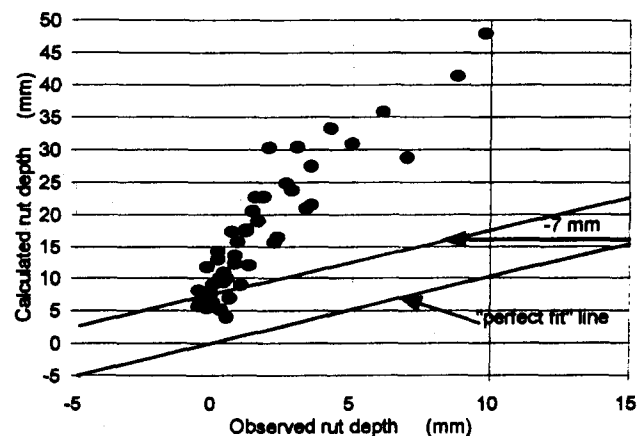


FIG. 10. Comparison of Corps of Engineers 1992 Equation Predictions for Rut Depth to Observed Rut Depths; Data for Wheel 4, 5–10 m Removed

strain causing ruts took place in the subgrade, rather than the subbase, and that the greatest vertical displacement occurred at the top of the subgrade.

The accuracy of the equation itself should be considered. The equation is the result of a multiple regression on the 273 observations of rut depth WES made. Although the values of input parameters used by WES span the data in the present study, (1) does not adequately predict values observed in the present study. However, the form of the equation does appear satisfactory given the high  $r^2$  value.

In the WES study, rut depth was defined as the difference between the lowest point in a rut and the road surface heave just beside it. In the current experiment, rut depth was defined as the lowering of the road surface from its original elevation before trafficking. With no heave being taken into account, observed rut depths as defined would always be less than or, at most, equal to the rut depth that would have been recorded using the WES definition.

The sources of the difference between the predictions of (1) and the observed data lie in the interpretation of ESWL, the coefficients of (1), which was based on far fewer observations than made in the current study, or the differing definitions of rut depth. The differing definitions for rut depth are thought to account for the largest portion of the difference.

## CONCLUSIONS

Within the range of wheel loads (44 and 80 kN), tire inflation pressures (345 and 690 kPa), subbase thicknesses (200, 350, and 560 mm), number of passes ( $N \leq 10,000$ ), and materials used in this project, the following can be concluded from the results of this phase of the project.

For all combinations of wheel load, tire inflation pressure, and subbase thickness, the rate of rut depth formation accelerated continuously up to 10,000 passes, at which point loading was discontinued (Figs. 3–5).

The lower inflation pressure generally produced flatter rut cross sections. The standard deviation of rut depth was 1.74 mm for the low inflation pressure and 2.11 mm for the high inflation pressure, over all data collected (Table 3).

Significantly shallower ruts formed when the tire inflation pressure was halved (345 kPa instead of 690 kPa) for a given subbase thickness and number of passes. The grand average for rut depth ratio was 0.56 for halving the tire inflation pressure (Table 4). This is equivalent to saying that ruts formed more slowly with trafficking in model roads subjected to the passage of tires with the lower inflation pressure.

Increasing the wheel load by 82% (80kN/44 kN = 1.82) resulted in ruts, on average, 5.7 times deeper for a given subbase thickness and number of passes. The grand average for rut depth ratio was 5.7 for increasing wheel load by 82% (Table 4).

While the form of the WES equation for the prediction of rut depth as a function of wheel load, tire inflation pressure, number of passes, subbase thickness, subbase CBR, and subgrade CBR appeared appropriate, it always overpredicted the observed rut depths (Fig. 10). Thus it is recommended that the equation be recast in terms of the more familiar 80-kN equivalent single axle loading.

## ACKNOWLEDGMENTS

The significant funding provided by the Canadian Natural Sciences and Engineering Research Council, through its Strategic Grants program, is greatly appreciated. The carefully considered input to the project proposal by collaborators at the Forest Engineering Research Institute of Canada (Vancouver and Montreal), the MacMillan Bloedel Company (Vancouver), Alberta Pacific Forest Products (Athabasca, Alberta), Weldwood Forest Industries (Hinton, Alberta), Repap Forest Industries (LePas,

Manitoba), J. D. Irving Ltd. (Saint John, New Brunswick), and the Newfoundland Department of Forestry and Agriculture contributed significantly to the success of the project. The consistently high professional standards exhibited by Tony Halliday and David Blackman at the Transport Research Laboratory are gratefully acknowledged. Finally, appreciation is expressed for the fruitful discussions with Andrew Dawson, Nottingham University.

## APPENDIX I. REFERENCES

- Amlin, E., and Bradley, A. H. (1992). "Variable tire pressure control for log-hauling vehicles." *Proc., Int. Mountain Logging and 8th Pacific Northwest Skyline Symp.*
- Ashmore, C., and Sirois, D. L. (1987). "Influences of the central tire inflation system on log truck performance and road surfaces." *Am. Proc., Soc. of Agric. Engrs. Annual Meeting*, Paper 87-1057.
- Bekker, M. G. (1956). *Theory of land locomotion, the mechanics of vehicle mobility*. The University of Michigan Press, Ann Arbor, Mich.
- Bradley, A. H. (1991). "Traction evaluation of a central tire inflation system." *Field Note Loading and Trucking-28*. Forest Engineering Research Institute of Canada, Vancouver, Canada.
- Bradley, A. H. (1992). "Reduction transportation costs with CTI systems." *Field Note Loading and Trucking-31*. Forest Engineering Research Institute of Canada, Vancouver, Canada.
- Bradley, A. H. (1993a). "Using variable tire pressure technology to reduce forest road costs." *Proc., Woodlands Section Ann. Meeting*. Canadian Pulp and Paper Association, Montreal, Canada.
- Bradley, A. H. (1993b). "Testing a CTI system in western log-hauling conditions." *Tech. Note TN-197*. Forest Engineering Research Institute of Canada, Vancouver, Canada.
- Czako, T. F. (1974). "The influence of the inflation pressure on cross-country performance." *Journal of Teramech.*, 11(3–4), 13–23.
- Della-Moretta, L. B. "Proof of concept tests for central tire inflation." U.S. Forest Service Equipment Development Center, San Dimas, Calif.
- Della-Moretta, L. B., and Hodges, H. C. (1983). "Off-highway tire/road damage and healing mechanisms." Proj. 8371 1202, U.S. Forest Service Equipment Development Center, San Dimas, Calif.
- Design guide: reduced inflation pressure limits for radial ply tubeless truck tires used off highway at reduced speed. Ref. 2-29-A* (1989). Tire and Rim Association, Inc., Akron, Ohio.
- Douglas, R. A. (1988). "Forest roads R&D, why it often fails us." *UNB Forestry Focus*, 13(4).
- Grau, R. W. (1993). "Effects of variable tire pressure on road surfacings." *Technical Report GL-93-20, Vol. I: design, construction, behavior under traffic, and test results*, U.S. Army Corps of Engineers, Waterways Experiment Station, Vicksburg, Miss.
- Greenfield, P. (1992). "CTI: the USDA Forest Service program." *Proc., 15th Annu. Meeting, Council on Forest Engrg. (CoFE)*.
- Murphy, G., and Martin, M. (1992). "Variable tire pressure activities in the southern region of the USDA Forest Service." *Proc., 15th Annu. Meeting, Council on Forest Engrg.*
- Smith, D. M. (1993). "Effects of variable tire pressure on road surfacings." *Tech. Rep. GL-93-20, Vol. II: Analysis of test results*. U.S. Army Corps of Engineers, Waterways Experiment Station, Vicksburg, Miss.
- Standard for central tire inflation system*. (1990). United States Forest Service.
- Taylor, D. J. (1987). *National central tire inflation program—Boise National Forest field operational tests*. Proj. 8771 1201, U.S. Forest Service Equipment Development Center, San Dimas, Calif.
- Taylor, D. J. (1988). *National central tire inflation program—Olympic National Forest field operational tests*. Proj. 8771 1201, U.S. Forest Service Equipment Development Center, San Dimas, Calif.
- United Kingdom Department of Transportation. (1991). *Manual of contract documents for highway works. Volume 1: Specifications for highway works. Series 800: road pavements, unbound materials*. Her Majesty's Stationery Office, London, U.K.

## APPENDIX II NOTATION

The following symbols are used in this paper:

- $C_1$  = CBR for subbase;  
 $C_2$  = CBR for subgrade;  
 $N$  = number of passes (experimental work);  
 $P_k$  = equivalent single wheel load (kips);  
 $R$  = number of passes (WES equation);  
 $RD$  = rut depth (inches);  
 $t$  = subbase thickness (inches); and  
 $t_p$  = tire inflation pressure (lb/in.<sup>2</sup>).